

# Kinematics of a grasping articulated mechanical hand

A. Bouachari\*, H. Tebbikh\*\*

\*Faculté de technologie, Université 20 Août 1955 Skikda, BP 26 Route El hadaek, Skikda, Algérie,

E-mail: a\_bouachari@hotmail.com

\*\*Automation and Computing Lab., Guelma Univ., PO Box 401, Guelma-24000, Algeria, E-mail: tebbikh@yahoo.com

**crossref** <http://dx.doi.org/10.5755/j01.mech.19.2.4148>

## 1. Introduction

The grasping of an object by a robotic hand is essentially a contact problem that may be represented by several closed loops, the object constituting the passive chain and the fingers the active one.

Great developments of articulated mechanical hands have been achieved. The Stanford-JPL hand is a mechanism constituted of three modular fingers that has not been designed for hominoid ends, but rather and mainly for handling purposes. Salisbury [1] reported later that to be more effective, the hand needs a fourth finger. The development of a four-finger hand has been carried out by the Massachusetts Institute of Technology [2] and the University of Utah [3]. It possesses a thumb opposing three long fingers, and has been the subject of interest in the field of teleoperation [4].

The present investigation focuses on both geometric models and kinematics of a four fingered robotized hand. Closed loop constraints are integrated whenever there is an object to be grasped.

The contact points are determined using the inverse geometric model of the active loop. Singularities as

well as any closed loop kinematics movement are analyzed by considering two fingers in any permutation.

The achieved simulation results are presented using object models build up by means of the superquadric approach developed by El-Khoury [5].

## 2. The articulated hand

The robotized hand is an articulated mechanical system constituted of a complex kinematics chains. The considered structure consists of four fingers (three long fingers opposing a thumb) having each four degrees of freedom (Fig. 1).

### 2.1. The direct geometrical model

To represent the geometric model of the fingers represented in Fig. 1, the parameters developed by Khalil and Kleinfinger [6], namely  $\alpha_j$ ,  $\sigma_j$ ,  $d_j$ ,  $\theta_j$ ,  $r_j$  allowing a uniform description and presented in Table 1 and Table 2 are adopted.

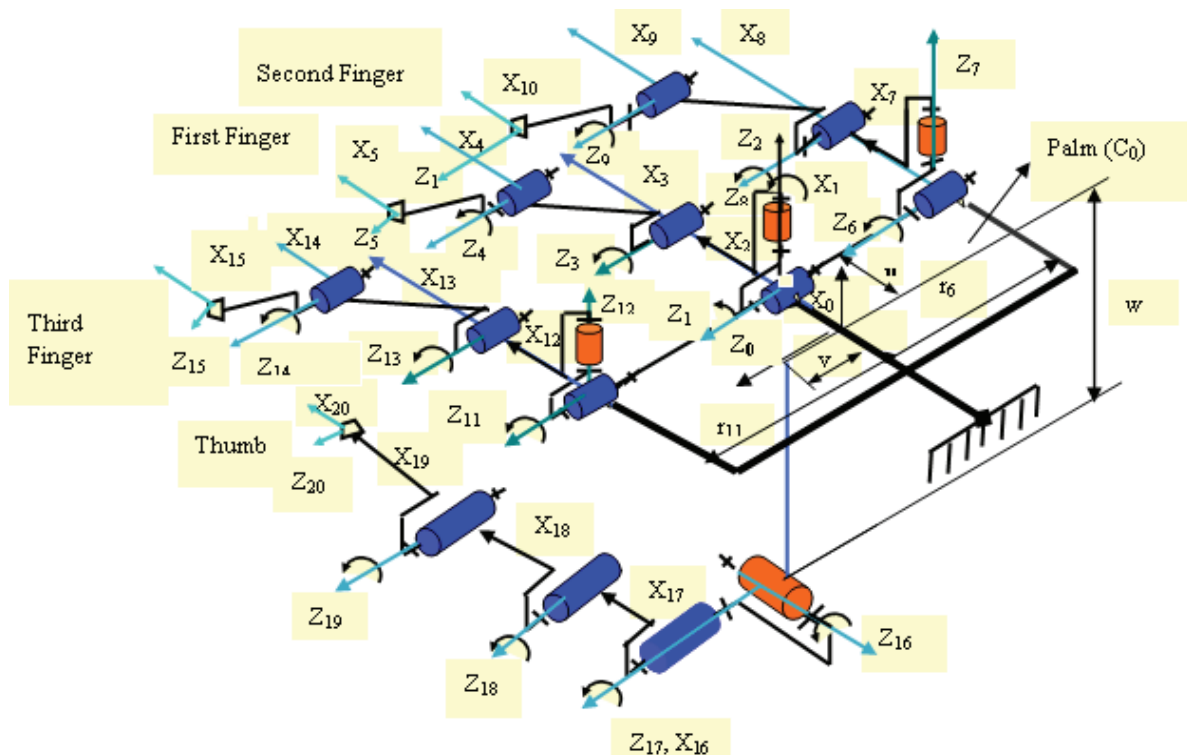


Fig. 1 Four fingered mechanical hand

Table 1  
Geometrical parameters of the prime long finger

$j$	$a(j)$	$\sigma_j$	$\alpha_j$	$d_j$	$\theta_j$	$r_j$
1	0	0	$-\pi/2$	$u$	$\theta_1$	0
2	1	0	$\pi/2$	0	$\theta_2$	0
3	2	0	$-\pi/2$	$d_3$	$\theta_3$	0
4	3	0	0	$d_4$	0	0

Table 2

Geometrical parameters of the thumb

$j$	$a(j)$	$\sigma_j$	$\alpha_j$	$d_j$	$\theta_j$	$r_j$	$\gamma_j$	$b_j$
16	0	0	$-\pi/2$	$v$	$\theta_{16}$	0	$\pi/2$	$-w$
17	16	0	$-\pi/2$	0	$\theta_{17}$	0	0	0
18	17	0	0	$d_{18}$	$\theta_{18}$	0	0	0
19	18	0	0	$d_{19}$	$\theta_{19}$	0	0	0
20	19	0	0	$d_{20}$	0	0	0	0

The different kinematics of the thumb need the addition of two new parameters to its description, namely

$\gamma_j$  and  $b_j$ . They are represented in Fig. 2.

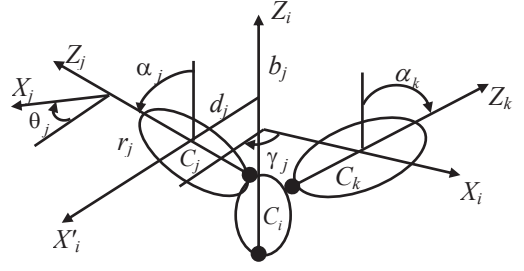


Fig. 2 Geometrical parameters representation [6]

The developed geometrical model in this paper is essentially based on an analysis performed earlier by Bouachari and Barkat [7]. Its application needs to start determining the antecedent of  $j$  namely  $i = a(j)$  before computing the transformation matrices  ${}^i T_j$  followed by their product  ${}^0 T_j$  ( $i = 0$  representing the center of the palm) to finally computing the position vectors corresponding to each of transformation matrix.

Fig. 3 shows three simulated configurations of our hand. They are represented by pinch grasp, normal grasp, and a grasp using the four fingertips. They have been achieved through the application of the direct geometrical model.

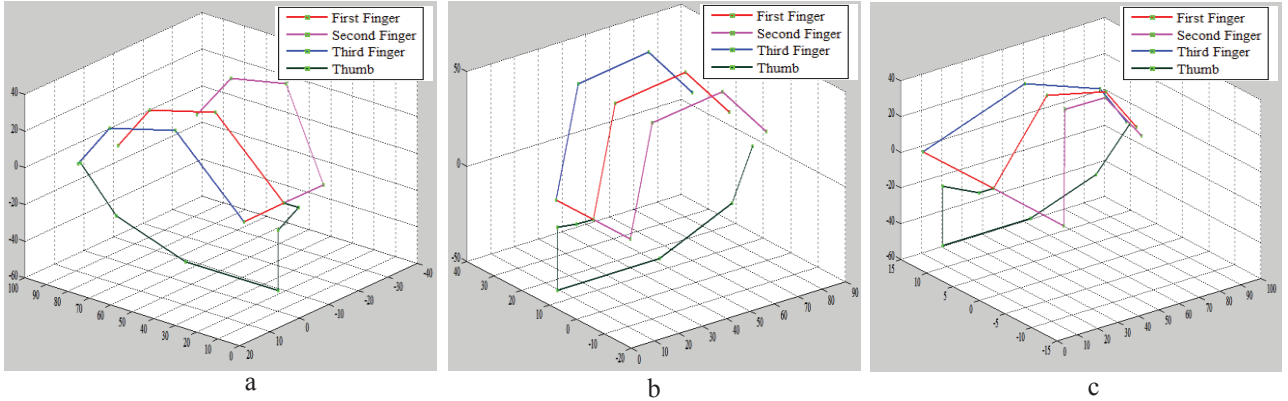


Fig. 3 Simulated configurations that are specific to a hominoid hand: a - pinch grasp; b - normal grasp; c - four finger tips grasp

## 2.2. The direct kinematical model

The kinematical model of a finger is represented by the fingertip velocity as a function of its joint velocities  $\dot{q}_{jk}$ . The basic Jacobian matrix is used to express the kinematics torsor  $\mathcal{G}_n$  in the coordinate system  $R_0$ :

$$\mathcal{G}_n = \begin{bmatrix} V_n \\ \omega_n \end{bmatrix} = J_n \dot{q}. \quad (1)$$

The corresponding Jacobian matrix is noted  ${}^0 J_n$  and its column  $k$  is expressed as:

$${}^0 J_{n,k} = \begin{bmatrix} \sigma_k {}^0 a_k + \bar{\sigma}_k {}^0 \bar{a}_k ({}^0 P_n - {}^0 P_k) \\ \bar{\sigma}_k {}^0 a_k \end{bmatrix}. \quad (2)$$

where the elements of each column are obtained when calculating the direct geometrical model of the matrices  ${}^0 T_k$  and vectors  ${}^0 P_n$  for the values of  $k$  from 1 to  $n$ .

The Jacobian matrix for each finger (noted  ${}^0 J_5, {}^0 J_{10}, {}^0 J_{15}, {}^0 J_{20}$ ) is therefore derived. For the first finger, it is expressed as:

$${}^0 J_5 = \begin{bmatrix} j_{1,1} & \cdots & j_{1,5} \\ \vdots & & \ddots \\ j_{6,1} & \cdots & j_{6,5} \end{bmatrix}. \quad (3)$$

The joint variable for each fingertip being equal to zero, the above expressed Jacobian matrices become  ${}^0 J_4, {}^0 J_9, {}^0 J_{14}$  and  ${}^0 J_{19}$ . This leads to expressing the basic Jacobian matrix (1) for the total number of fingers.

By expressing the Jacobian matrix of Eq. (4) as the product of two sub-matrices  ${}^0JT_4 {}^0JR_4$ , one can compute the fingertip translational velocity vector  ${}^0V_5$  in the coordinate system  $R_0$  linked to the hand palm through the sub-matrix  ${}^0JT_4$  of dimensions  $(3 \times 4)$ :

$$\begin{bmatrix} {}^0V_{5,x} \\ {}^0V_{5,y} \\ {}^0V_{5,z} \\ {}^0\omega_{5,x} \\ {}^0\omega_{5,y} \\ {}^0\omega_{5,z} \end{bmatrix} = \begin{bmatrix} j_{1,1} & \cdots & j_{1,4} \\ \vdots & & \ddots \\ j_{6,1} & \cdots & j_{6,4} \end{bmatrix} \begin{bmatrix} \dot{q}_1 \\ \dot{q}_2 \\ \dot{q}_3 \\ \dot{q}_4 \end{bmatrix}; \quad (4)$$

$${}^0V_5 = \begin{bmatrix} {}^0V_{5,x} \\ {}^0V_{5,y} \\ {}^0V_{5,z} \end{bmatrix} = [{}^0JT_4] \begin{bmatrix} \dot{q}_1 \\ \dot{q}_2 \\ \dot{q}_3 \\ \dot{q}_4 \end{bmatrix}. \quad (5)$$

The sub-matrix  ${}^0JR_4$  leads to the computation of the fingertip rotational velocity vector  ${}^0\omega_5$  in the coordinate system  $R_0$  linked to the hand palm and is also of dimensions  $(3 \times 4)$ :

$${}^0\omega_5 = \begin{bmatrix} {}^0\omega_{5,x} \\ {}^0\omega_{5,y} \\ {}^0\omega_{5,z} \end{bmatrix} = [{}^0JR_4] \begin{bmatrix} \dot{q}_1 \\ \dot{q}_2 \\ \dot{q}_3 \\ \dot{q}_4 \end{bmatrix}. \quad (6)$$

The Jacobian matrix is computed under Maple using Eq. (2).

### 3. Singular configurations specification

To define the singular configurations of the hand, the theory of Singular Value Decomposition developed by Brown and Vardy [8] is applied. It implies the decomposition of the Jacobian matrix into two sub-matrices of dimensions  $(4 \times 3)$  for each finger, one for the translation movement noted  $({}^0JT_j)_h$  and the other for the rotation movement  $({}^0JR_j)_h$ . Each matrix can be decomposed further into a product of three matrices involving the singular values. The rotation matrix  $({}^0JR_j)_h$  being of dimension  $(4 \times 3)$ , it may be expressed as the product of three orthogonal matrices  $U$ ,  $V$  and  $S_j$  of dimension  $(4 \times 4)$ ,  $(3 \times 3)$  and  $(4 \times 3)$  respectively. It comes:

$$({}^0JR_j)_h = (U_j \ S_j \ V_j^T)_h, \quad (7)$$

$$\text{with } S_j = \begin{bmatrix} (\Delta_j)_h & 0 \end{bmatrix}. \quad (8)$$

$(\Delta_j)_h$  is a  $(3 \times 3)$  diagonal matrix constituted by

the non-zero singular values  $\sigma_i$  of the Jacobian matrix of rotation arranged in decreasing order. The singular values of  $({}^0JR_j)_h$  represent in fact the square roots of the Eigen values of the product  $({}^0JR_j)_h^T ({}^0JR_j)_h$ . Therefore:

$$\det(\Delta_j)_h = \prod_j \sigma_i. \quad (9)$$

The computation of the rotation matrix for the first finger under Maple gives (where  $S$  and  $C$  stand for sine and cosine respectively):

$$({}^0JR_j)_h = \begin{bmatrix} 0 & Sq_1 & -Cq_1Sq_2 & -Cq_1Sq_2 \\ 1 & 0 & Cq_2 & Cq_2 \\ 0 & Cq_1 & Sq_1Sq_2 & Sq_1Sq_2 \end{bmatrix}; \quad (10)$$

$$\text{with } \begin{cases} \sigma_1 = \sqrt{\frac{3}{2} + \frac{1}{2}(\sqrt{1+Cq_2^2})}; \\ \sigma_2 = 1; \\ \sigma_3 = \sqrt{\frac{3}{2} - \frac{1}{2}(\sqrt{1+Cq_2^2})}, \end{cases} \quad (11)$$

$$\text{leading to: } (\Delta_j)_h = \begin{bmatrix} \sigma_1 & 0 & 0 \\ 0 & \sigma_2 & 0 \\ 0 & 0 & \sigma_3 \end{bmatrix}. \quad (12)$$

The singular positions of the first finger correspond to the nullification of the determinant of the matrix  $(\Delta_j)_h$  leading to  $\sigma_3 = 0$  and therefore  $\cos(q_2) = 0$ . The same procedure is applied to all fingers.

For the long fingers, this means:  $\cos(q_7) = 0$  and  $\cos(q_{11}) = 0$ . For the thumb, the corresponding matrix can be shown to be:

$$({}^0JR_j)_h = \begin{bmatrix} -1 & 0 & 0 & 0 \\ 0 & Cq_{16} & Cq_{16} & Cq_{16} \\ 0 & 0 & 0 & 0 \end{bmatrix}. \quad (13)$$

The computation of the corresponding singular positions for the thumb requires  $\cos(q_{16}) = 0$ . In this case, the thumb does not present any singularities since these are usually independent of the first joint. It is noticed that a unique singular configuration shows up for each finger, and leads to a singular layout for the whole hand.

Four different simulations have been carried out and are presented in Fig. 4:

- $(q_1, q_2, q_{12}) = \pm\pi/2$ : The long fingers are folded up over the palm in both directions (Fig. 4, a);
- $q_2 = \pm\pi/2$ : The first finger folded up over the palm (Fig. 4, b);
- $q_7 = \pm\pi/2$ : The second finger folded up over the palm in both directions (Fig. 4, c);
- $q_{12} = \pm\pi$ : The third finger folded up over the palm in both directions (Fig. 4, d).

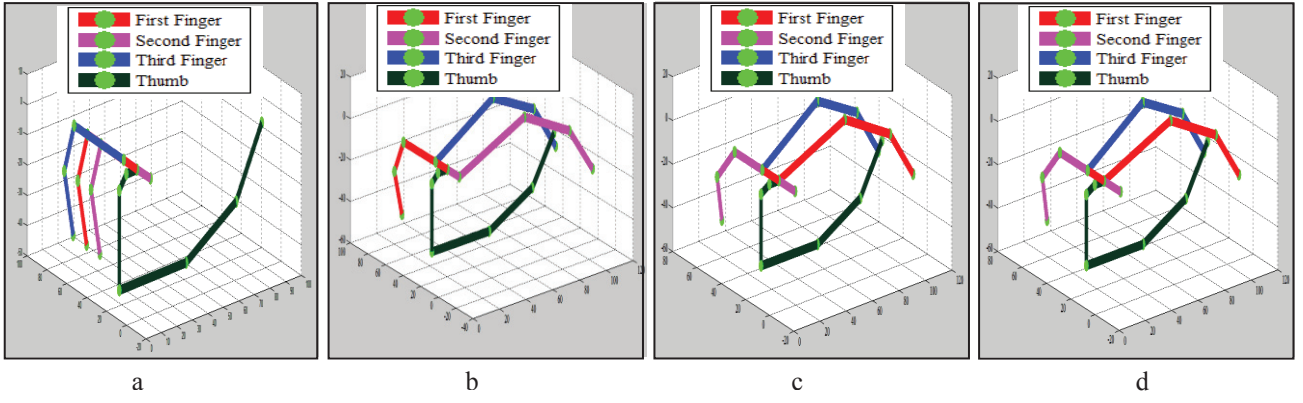


Fig. 4 Singular configurations: a - full hand; b - first finger; c -second finger; d - third finger

#### 4. Hand-object kinematical movement processing

The processing of the system hand-object involves necessarily loops. When a number of  $N$  objects are grasped using  $n$  fingers for example, a number of  $(n-1)$  kinematics loops are involved as stated by El-Khoury [5] and Rosales et al [9]. The equation needed for the closure of the system and incorporating loops taken in pairs in any permutations, leads to a vanishing torsor. This relationship is obtained through expressing the velocities relation at a reduction station. For a vanishing torsor, this condition can be expressed independently of any projection coordinate system as shown by El-Khoury [5]:

$$\sum_{i=1}^{n-1} \mathcal{G}_{i,i+1}^o + \mathcal{G}_{n,1}^o = 0. \quad (14)$$

A linear relationship links the kinematics torsor and the derivative of the configuration vector noted  $\dot{Q}_{i,j}$ .

Taking into account the straight path of the loop ( $i$  towards  $j$ ,  $i$  and  $j$  indicating the fingers), this relationship may be obtained through expressing the kinematics torsor at station  $i$ . This leads to:

$$V_{i,j}^i = \begin{bmatrix} I_3 & 0 \\ 0 & J_{oi,j} \end{bmatrix}, \quad (15)$$

where  $I_3$  and  $J_{oi,j}$  refer to the identity matrix and the  $(3 \times n)$  Jacobian sub-matrix used to compute the velocity of rotation respectively.

The combination of Eqs. (14) and (15) requires the computation of the velocity for each contact point of fingers  $i$  and  $j$ . If it is traversed in the forward direction, the corresponding relative velocity should be computed at  $i$  through the application of the point switching classical relationship at this particular point. Eqs. (16) and (17) are obtained for the cases of the direct and indirect paths respectively:

$$V_{i,j}^o = \begin{bmatrix} I_3 & \tilde{O}_i \\ 0 & I_3 \end{bmatrix} V_{i,j}^i; \quad (16)$$

$$V_{i,j}^o = - \begin{bmatrix} I_3 & \tilde{O}_j \\ 0 & I_3 \end{bmatrix} V_{i,j}^i, \quad (17)$$

where  $\tilde{O}_x$  represents the vector pre-product matrix.

The first first-order approximation of the derivative of the configuration vector may be expressed as:

$$\dot{Q}_{i,i+1} = \frac{\Delta Q_{i,i+1}}{\Delta t}. \quad (18)$$

Introducing a Boolean variable that equals unity or zero if it is traversed in the forward or reverse directions respectively, and combining the above Eqs. (15)-(18) leads to the exact variational formulation of the strain relationship which is linear with respect to the increment  $\Delta Q$  (Eq. 19).

In addition to the Jacobian rotation sub-matrix  $J_{oi,j}$ , the use of the sub-matrix of translation  $J_{vij}$  allows for the reformulation of the strain relationship Eq. (19):

$$\sum_{i=1}^{n-1} S - \left\{ \begin{bmatrix} I_3 & \hat{O}_i J_{oi,i+1} \\ 0 & J_{oi,i+1} \end{bmatrix} - \bar{S} \begin{bmatrix} I_3 & \hat{O}_{i+1} J_{oi,i+1} \\ 0 & J_{oi,i+1} \end{bmatrix} \right\} \Delta Q_{i,i+1} + \left\{ \begin{bmatrix} I_3 & \hat{O}_n J_{on,1} \\ 0 & J_{on,1} \end{bmatrix} - \bar{S} \begin{bmatrix} I_3 & \hat{O}_1 J_{on,1} \\ 0 & J_{on,1} \end{bmatrix} \right\} \Delta Q_{n,1} = 0. \quad (19)$$

The factorization of the Jacobian is justified in the literature by diverse contact models leading to the grasping of objects [10]. Three basic contact types may be defined. Both the first and second types use the Jacobian rotation sub-matrix to formulate the kinematics torsor. However, while the first case does not allow for any fingertips slipping or rolling (Eq. 20), the second one allows solely for fingertips rolling (Eq. 21):

$$\begin{cases} [V_x & V_y & V_z]^T = 0; \\ [\omega_x & \omega_z]^T = 0; \end{cases} \quad (20)$$

$$\begin{cases} [V_x & V_y & V_z]^T = 0; \\ \omega_z = 0. \end{cases} \quad (21)$$

The third and last contact type uses the Jacobian translation sub-matrix, and allows for fingertips slipping only. The kinematics torsor is expressed as:

$$\begin{cases} V_z = 0; \\ [\omega_x & \omega_y & \omega_z]^T = 0. \end{cases} \quad (22)$$

5. Applications to object grasping

Table 3

The closure constraint expressed by Eq. (20) may be applied to specific types of grips [11]. In this case, the objects are held between the fingertips while the thumb is placed in opposition.

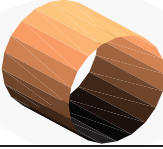
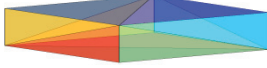
It has to be acknowledged that most studies involving the grasping of an object imply a simplified representation of it based on an extension of the superquadrics i.e. the superellipsoïdes which possess the following implicit form:

$$f(x, y, z) = \left( \left( \frac{x}{a_1} \right)^{\frac{2}{\varepsilon_2}} + \left( \frac{y}{a_2} \right)^{\frac{2}{\varepsilon_2}} \right)^{\frac{\varepsilon_2}{\varepsilon_1}} + \left( \frac{z}{a_3} \right)^{\frac{2}{\varepsilon_1}}, \quad (23)$$

where  $a_1, a_2$  and  $a_3$  define the scale factor on the coordinates axes  $x, y$  and  $z$  respectively;  $\varepsilon_1$  and  $\varepsilon_2$  define the curvature in the  $(x, y)$  and  $(x, z)$  directions;  $f(x, y, z) = 1$  if the point  $(x, y, z)$  is situated on the body surface;  $f(x, y, z) < 1$  if the point  $(x, y, z)$  is situated inside the body;  $f(x, y, z) > 1$  if the point  $(x, y, z)$  is situated outside the body.

The above listed conditions enable the description of a wide spectrum of shapes ranging from simple ellipsoids ( $\varepsilon_1 = \varepsilon_2 = 1$ ), parallelepipeds ( $\varepsilon_1 \rightarrow 0$  and  $\varepsilon_2 \rightarrow 0$ ) and cylinders ( $\varepsilon_1 = 1$  and  $\varepsilon_2 \rightarrow 0$ ). They have been uti-

Diverse modeled objects to be grasped

Superellipsoïdes	$\varepsilon_1$	$\varepsilon_2$
	1	1
	0.1	1
	0.1	0.1

zed to model the objects represented in Table 3.

Moreover, when the last condition ( $f(x, y, z) > 1$ ) is corroborated, the specific requirements to the first joint of each finger used in the inverse geometric model have to be integrated.

Three different grasping types have been investigated. They are represented in Figs. 5-9.

The first case illustrated in Fig. 5 presents a sphere being grasped using fingertips while the thumb is placed in opposition. The data obtained through the inverse geometrical model used to describe this configuration as well as the variable joints are summarized in Table 4 (positions are expressed in mm) and Table 5 respectively.

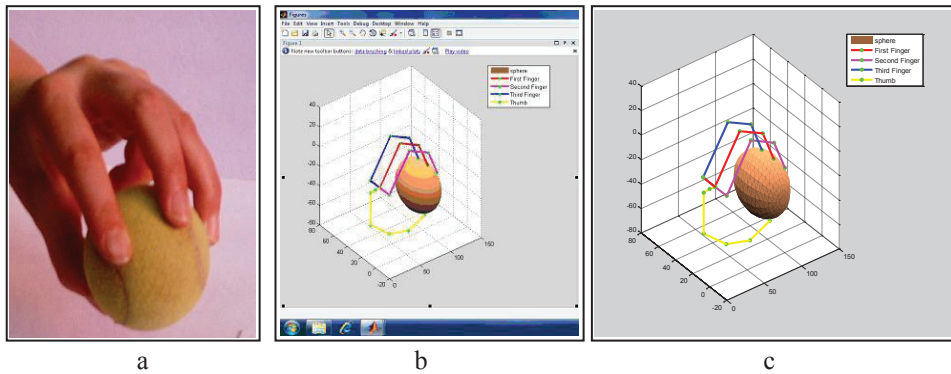


Fig. 5 Fingertips sphere grasping: a - illustration; b - graphical representation; c - results representation

Table 4

Inverse Geometrical Model (MGI) data for fingertips grasping of a sphere

Initial positions relatively to the palm							
Finger 1		Finger 2		Finger 3		Thumb	
$p_{x1}$	120.59	$p_{x2}$	102.60	$p_{x3}$	102.60	$p_{x4}$	93.06
$p_{y1}$	0.00	$p_{y2}$	-15.00	$p_{y3}$	15.00	$p_{y4}$	7.00
$p_{z1}$	16.40	$p_{z2}$	-16.46	$p_{z3}$	-16.47	$p_{z4}$	-42.84
Specific conditions relatively to 1st joint							
Finger 1		Finger 2		Finger 3		Thumb	
$p_{11}$	82.02	$p_{21}$	82.03	$p_{31}$	82.03	$p_{41}$	93.06
$p_{12}$	51.78	$p_{22}$	51.77	$p_{32}$	51.78	$p_{42}$	7.00
$p_{13}$	0.00	$p_{23}$	0.00	$p_{34}$	0.00	$p_{42}$	-52.84
Specific conditions relatively to 2nd joint For the thumb							
$p_{x2}$		$p_{y2}$		$p_{z2}$			
81.99		44.12		0.00			

Table 5

The joint variables of a sphere grasping

Finger 1	Finger 2	Finger 3
$q_1 = -22^\circ 28'$	$q_6 = -22^\circ 28'$	$q_{11} = -22^\circ 28'$
$q_2 = 44^\circ 58'$	$q_7 = 44^\circ 58'$	$q_{12} = 44^\circ 58'$
$q_3 = 44^\circ 58'$	$q_8 = 44^\circ 58'$	$q_{13} = 44^\circ 58'$
$q_4 = 29^\circ 59'$	$q_9 = 29^\circ 59'$	$q_{14} = 29^\circ 59'$
$q_5 = 0$	$q_{10} = 0$	$q_{15} = 0$
Thumb		
$q_{16} = 89^\circ 57'$		
$q_{17} = 61^\circ 52'$		
$q_{18} = 30^\circ 55'$		
$q_{19} = 41^\circ 13'$		
$q_{20} = 0$		

Table 6

The joint variables of a cylinder grasping

Finger 1	Finger 2	Finger 3
$q_1 = -22^\circ 29'$	$q_6 = 22^\circ 23'$	$q_{11} = -22^\circ 10'$
$q_2 = 0$	$q_7 = -12^\circ$	$q_{12} = 44^\circ 58'$
$q_3 = 44^\circ 57'$	$q_8 = 44^\circ 58'$	$q_{13} = 44^\circ 58'$
$q_4 = 29^\circ 59'$	$q_9 = 29^\circ 58'$	$q_{14} = 29^\circ 59'$
$q_5 = 0$	$q_{10} = 0$	$q_{15} = 0$
Thumb		
$q_{16} = 89^\circ 57'$		
$q_{17} = 61^\circ 52'$		
$q_{18} = 30^\circ 55'$		
$q_{19} = 41^\circ 13'$		
$q_{20} = 0$		

Table 7

The joint variables of a parallelepiped grasping

Finger 1	Finger 2	Finger 3
$q_1 = -22^\circ 29'$	$q_6 = 22^\circ 23'$	$q_{11} = -22^\circ 10'$
$q_2 = 0$	$q_7 = -12^\circ$	$q_{12} = 12^\circ$
$q_3 = 44^\circ 57'$	$q_8 = 44^\circ 58'$	$q_{13} = 44^\circ 54'$
$q_4 = 29^\circ 59'$	$q_9 = 29^\circ 58'$	$q_{14} = 29^\circ 53'$
$q_5 = 0$	$q_{10} = 0$	$q_{15} = 0$
Thumb		
$q_{16} = 90^\circ$		
$q_{17} = 53^\circ 46'$		
$q_{18} = 21^\circ 25'$		
$q_{19} = 29^\circ 59'$		
$q_{20} = 0$		

The second and third cases illustrating the fingertips grasping of a cylinder and a parallelepiped follow the same procedure. For the cylinder, Table 6 summarizes the results of the inverse geometrical model application while Figs. 6 and 7 represent the grasping of this geometry using the tips of the fingers. For the parallelepiped, Table 7 and Figs. 8 and 9 present the results obtained and fingertips grasping respectively.

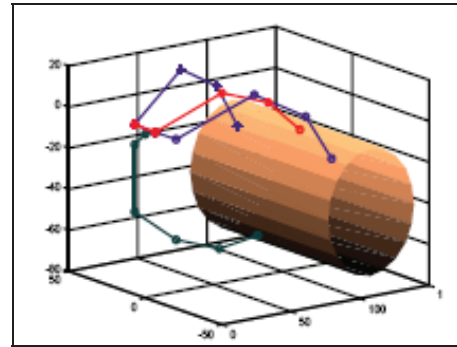


Fig. 7 Graphical representation of a cylinder grasping

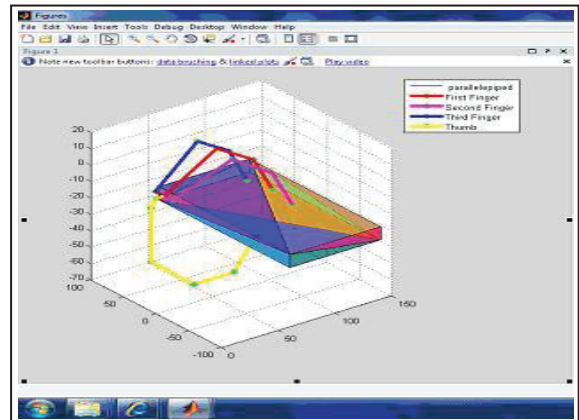


Fig. 8 Simulation of a parallelepiped grasping

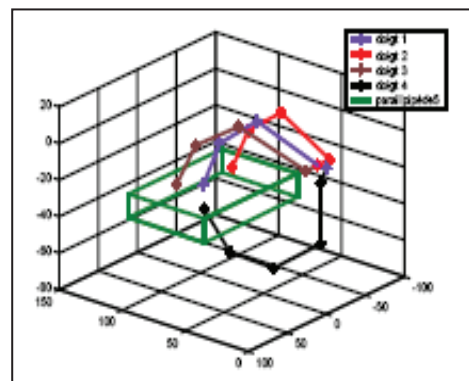


Fig. 9 Graphical representation of parallelepiped grasping

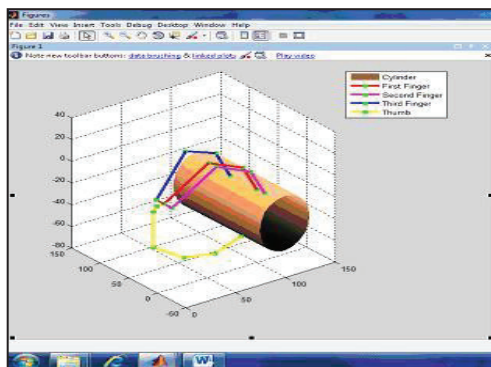


Fig. 6 Simulation of a cylinder grasping

## 6. Conclusions

The present paper investigates the theoretical approaches concerning the grasping of diverse objects using a robotized hand consisting of four fingers. The study of grasping leads us to the modeling of articulated systems working in closed loop.

The inverse geometrical model is applied to determining the contact points of the fingers with the object under consideration, while the kinematics model is used to

highlighting the singular configurations of the fingers. The problem associated to singularities is treated first for the case of free motion.

The hand Jacobian matrix singular value decomposition approach is carried out to determining the singularities occurring close to the contacts considered.

Finally, the approach developed is applied to simulating the grasping of diverse objects using the robotized hand and the results obtained presented.

### Acknowledgements

The authors wish to acknowledge the contribution of Professor A Haddad from Taibah University for his useful suggestions and review which enhanced the quality of this work.

### References

1. **Design News**. 1985. Robot grippers gain dexterity-End effectors under development enable robots to grasp and manipulate objects with the gripper much like the human hand, 3-18-85.
2. **Mason, M.T.; Salisbury, J.K.** 1985. Robot hands and the mechanics of manipulation, MIT Press.
3. **Jacobsen, S.C.; Iversen, E.K.; Knutti, D.F.; Johnson, R.T.; Biggers, K.B.** 1986. Design of the UAT/MIT. Dexterous Hand, Engineering Design Center, University of Utah, 1520-1532.
4. **Gallaf, A.I.** 1997. Manipulation at ILL-conditioned configurations by a robot hand, Pergamon Mechatronics 7(5): 479-503.  
[http://dx.doi.org/10.1016/S0957-4158\(97\)00012-3](http://dx.doi.org/10.1016/S0957-4158(97)00012-3).
5. **El-Khoury, S.** 2008. Approche Mixte, Analytique et par Apprentissage pour la Synthèse d'une Prise Naturelle. PhD Thesis, Pierre and Marie-Curie University, 130-136.
6. **Khalil, W.; Dombre, E.** 1999. Modélisation, identification et commande des robots, HERMES Science Publications, Paris, France, 173-175.
7. **Bouachari, A.; Barkat, B.** 2005. Modélisation Géométrique d'une Main Mécanique Articulée Non-Anthropomorphe à Quatre Doigts, 1st International Congress on Design and Modeling of Mechanical Systems, CMSM'2005, Monastir-Tunisia.
8. **Brown, E.; Vardy, A.** 1998. Articulated human hand model with inter-joint dependency constraints, Computer Science 6752, Computer Graphics, Project Report, 8-9.
9. **Rosales, C.; Porta, J.M.; Suarez, R.; Ros, L.** 2008. Finding all valid hand configurations for a given precision grasp, IEEE International Conference on Robotics and Automation, Pasadena, USA, 1636-1640.
10. **Joseph, C.; Liu, C.Y.** 2001. Dynamic simulation of multi-fingered robot hands based on a unified model, robotics, Autonomous Systems, 32: 185-200.
11. **Aleotti, J.; Caselli, S.** 2010. Interactive teaching of task-oriented robot grasps, Robotics and Autonomous Systems, 58: 539-550.  
<http://dx.doi.org/10.1016/j.robot.2010.01.004>.

A. Bouachari, H. Tebbikh

### GRIEBIANČIOSIOS LANKSTINĖS MECHANINĖS RANKOS KINEMATIKA

#### R e z i u m ė

Pateiktas tyrimas susijęs su roboto rankos geometrinės ir kinematinės būsenos išsišakojimų sistemos įvertinimu. Uždaro kontūro apribojimai integruojami prieš pat objekto sugriebimą. Siekiant pabrėžti ypatumus, roboto rankos kinematinė analizė atliekama esant laisvam bekontaktčiam judesiui. Įvairių kinematinų apribojimų, atitinkančių skirtingus kontaktavimo atvejus, analizė atliekama vėliau. Kontaktavimo taškai nustatomi naudojantis aktyviosios grandies atvirkštinio geometrinio modeliu. Galiausiai tyrimas iliustruojamas konkrečiu rankos su keturiais pirštais, įgalinančiais sugriebti skirtingus objektus, taikymu.

A. Bouachari, H. Tebbikh

### KINEMATICS OF A GRASPING ARTICULATED MECHANICAL HAND

#### S u m m a r y

The present investigation deals with the representation of the geometrical and kinematical states of a robotic hand constituted from an arborescent system. Closed loops Constraints are integrated whenever a capture of objects is confronted. In order to highlight the singularities, the hand kinematical analysis is carried out in free movement without contact. The incorporation of the various kinematical constraints corresponding to different types of contact are studied afterwards. The contact points are determined through the application of the inverse geometric model of the active chain. Finally, the study is illustrated with an application consisting of a hand with four fingers enabling the grasping of diverse objects.

**Keywords:** articulated hand, grasping, contact kinematics, superquadric approach.

Received February 07, 2012

Accepted March 25, 2013